# Multiple Impact Factor Based Accuracy Analysis for Power Quality Disturbance Detection

Zijing Yang, Haochen Hua, and Junwei Cao

*Abstract*—Nowadays, power quality problems are affecting people's daily life and production activities. With the aim to improve disturbance detection accuracy, a novel analysis approach based on multiple impact factors is proposed in this paper. First, a multiple impact factors analysis is implemented in which two perspectives, i.e., the wavelet analysis and disturbance features are considered simultaneously. Five key factors, including wavelet function, wavelet decomposition level, redundant algorithm, event type and disturbance intensity, start and end moment of disturbance, have been considered. Next, an impact factors based accuracy analysis algorithm is proposed, through which each factor's potential impact on disturbance location accuracy is investigated. Three transforms, i.e., the classic wavelet, lifting wavelet and redundant lifting wavelet are employed, and their superiority on disturbance location accuracy is investigated. Finally, simulations are conducted for verification. Through the proposed method, the wavelet based parameters can be validly selected in order to detect power quality disturbance accurately.

*Index Terms*—Power quality, disturbance location accuracy, wavelet analysis, impact factors.

## NOMENCLATURE

| | |
|---|---|
| AMM | Amplitude of modulus maxima. |
| CWT | Continuous wavelet transform. |
| DWT | Discrete wavelet transform. |
| HPF | High pass filters. |
| LPF | Low pass filters. |
| LWT | Lifting wavelet transform. |
| PQ | Power quality. |
| RLWT | Redundant lifting wavelet transform. |
| $A$ | Voltage amplitude. |
| $a_j$ | Approximation coefficients at level $j$. |
| $d_j$ | Detailed coefficients at level $j$. |
| $j$ | Wavelet decomposition level. |
| $N$ | Vanishing moment order. |
| $t_{start}$ | Start moment of disturbance. |
| $t_{end}$ | End moment of disturbance. |
| $\alpha$ | Disturbance intensity. |

This work is supported by the National Natural Science Foundation of China (Grant No.61501040), Beijing Key Laboratory of Digital Printing Equipment, National Key Research and Development Program of China (Grant No. 2017YFE0132100) and BNRist Program (Grant No. BNR2020TD01009).

Z. Yang is with the College of Electromechanical Engineering, Beijing Institute of Graphic Communication, Beijing, 102600, P. R. China.

H. Hua is with the College of Energy and Electrical Engineering, Hohai University, 211100, P. R. China. (Corresponding Author: Haochen Hua, huahc16@tsinghua.org.cn)

J. Cao is with the Beijing National Research Center for Information Science and Technology, Tsinghua University, Beijing, 100084, P. R. China.

## I. INTRODUCTION

IN recent years, accompanied with the development of energy Internet [1], the trend of utilizing renewable energy has been increasing. Within the scope of energy Internet, the access of large-scale renewable energy resources would pose greater challenges to the governance of PQ [2]. In order to guarantee a stable voltage supply and to avoid economic loss, PQ is of great significance to the end users [3]-[5]. Disturbance, as one of the typical transient PQ problems, must be precisely detected for voltage regulation [6], [7]. Since disturbance would lead to short-term voltage deviation, effective recognition of signal's local discontinuous points is the key to disturbance detection.

To realize signal singularity detection, the wavelet analysis is widely adopted [8], [9]. The wavelet modulus maxima method, which is the key to detect signal's discontinuous points, has been applied to PQ disturbance detection [10]. However, given the fact that the classical wavelet is usually constructed in the frequency domain, and the transform depends on convolution that would increase computational complexity, significant advances on LWT have been made; see, e.g., [11], [12]. LWT can be realized in the time domain, so as to save computational cost, and its application for PQ disturbance identification has been paid close attention. In addition, other methods such as the empirical wavelet transform [13]-[15] and the complex wavelet [16] have been developed for PQ disturbance detection. By applying DWT or LWT to PQ issues, research on disturbance detection and classification has been extensively studied. In [17], to detect islanding and PQ disturbances, the db4 wavelet (see Appendix A) is adopted for decomposition, with corresponding results compared with that of the S-transform. In [18], wavelet packet combined with Tsallis singular entropy is utilized to detect five transient disturbance signals, and the db10 wavelet (see Appendix A) is employed through experiments. In order to identify PQ events accurately, ten optimal wavelets are selected for each machine learning algorithm from a total 110 base wavelets by proposing a direct and indirect approach [19]. In [20], to detect disturbance's start and end moment, wavelet decomposition at different levels is implemented to obtain detailed coefficients. In [21] and [22], the wavelet function and decomposition level are selected, such

that the feature extraction of disturbance has been realized. For PQ events detection, in [23], the db4 wavelet has been found to be better than db8 and fractionally designed, and the decomposition is employed up to fifth level. Aiming at conducting real-time recognition of PQ disturbances, the db4 wavelet and a six-level multiresolution analysis are selected for the signal processing module in [24], and the maximal overlap wavelet packet transform is presented in [25] with its performance evaluated with various wavelets. In [26], the generalized morphological open-closing and close-opening undecimated wavelet is put forward, together with a three levels decomposition applied, in which sense the PQ disturbances identification is implemented.

Reliable PQ disturbance detection is of great importance to stable power supply and industry, and the research of wavelet analysis on PQ disturbance detection has been widely studied. However, most of the research focuses on feature extraction and classification of PQ disturbance based on wavelet's multi-resolution analysis [17]-[26], and it is notable that the research on location accuracy of disturbance's start and end moment, which mainly bases on the singularity detection performance of wavelet and is one of the key issues in the field of voltage control, has not been fully investigated. The motivation of this paper is to locate disturbance's start and end moment more accurately in order to realize better power problem solving. The difficulty of achieving the aim lies on figuring out the reasons for location error occurring and explore an effective approach to improve disturbance location accuracy. Inspired by previous work, e.g., [20]-[22] in which parameter selection issues related to wavelet method or disturbance features are discussed to detect PQ disturbances and the analyzing methods presented in [27]-[29], a novel multiple impact factors based approach for accurate PQ disturbance location is proposed in this paper. First, a multiple impact factors analysis is conducted, in which the selection of factors that may influence location accuracy is investigated. Then, an impact factors based accuracy analysis algorithm is proposed, so as to investigate each factor's impact on disturbance location accuracy. Finally, simulations are implemented for validation.

The importance and main contributions of this paper can be highlighted as follows:

1. A novel multiple impact factors based approach for accurate power quality disturbance location is proposed. Two perspectives including the wavelet analysis and PQ disturbance features are considered simultaneously.

2. Five key factors are carefully considered, and each factor's potential impact on PQ disturbance location accuracy is investigated, separately. In this sense, the aim of optimal parameters selection in this paper is to achieve more accurate and flexible disturbance location, which is different from previous literatures (e.g., [17]-[22]) where parameters selection is investigated for feature extraction or classification.

3. Through the proposed impact factors based accuracy analysis algorithm, guidance on optimal selection of multiple parameters can be provided for disturbance location analysis and its hardware implementation, in which sense better disturbance detection can be realized compared to the method of single parameter optimal selection, e.g., [26], [29], [30].

## II. Preliminary

To clearly illustrate the proposed multiple impact factors approach, related wavelet theory is introduced in this section.

### A. Wavelet Modulus Maxima Based Disturbance Detection

The location of PQ disturbance's start/end moment is indeed the singularity detection problem, which can be solved by the wavelet modulus maxima method [31]. Such method can be illustrated as follows. For a low-pass smooth function $\theta(x)$ that satisfies $\int_{-\infty}^{\infty}\theta(t)dt = 1$ and $\lim_{|t|\to\infty}\theta(t) = 0$, its first derivative which is denoted as $\theta^1(x)$ is a wavelet. For any $j$, let $\theta_j(x) = (1/j)\theta(x/j)$. Then, the wavelet transform of a real function $f(x)$ and $\theta_j^1(x)$ is

$$W^1 f(j,x) = f * \left(j\, d\theta_j/dx\right)(x) = j\, d\left(f * \theta_j(x)\right)/dx. \quad (1)$$

In this sense, the wavelet transform $W^1 f(j,x)$ is the first derivative of $f(x)$ smoothed by $\theta_j(x)$.The local maxima of $|W^1 f(j,x)|$ corresponds to the sharp variation points of $f(x)$. Hence, the wavelet modulus maxima method can be used for signal's singularity detection. Based on this, two aspects are considered for PQ disturbance detection in this paper:

i. Location accuracy of disturbance's start and end moment. Higher disturbance location accuracy would be achieved when the disturbance location result is closer to the actual situation.

ii. The AMM of the located moment. It is more flexible to locate disturbance when the AMM is higher.

### B. Wavelet Analysis

In order to provide basis for the multiple impact factors analysis in Section III, basic theory of wavelet analysis is given as follows.

A function $\psi(x)$ within the square integral space $L^2(R)$ satisfying the admissibility condition

$$C_\psi = \int_R |w|^{-1}\left|\hat{\psi}(x)\right|^2 dw < \infty \quad (2)$$

is called mother wavelet [32].

With HPF and LPF corresponding to the wavelet function, DWT decomposition can be illustrated in Fig. 1. For a giving $j$, the signal can be decomposed level by level until the $j$-th level, such that $a_j$ and $d_j$ can be obtained [33].

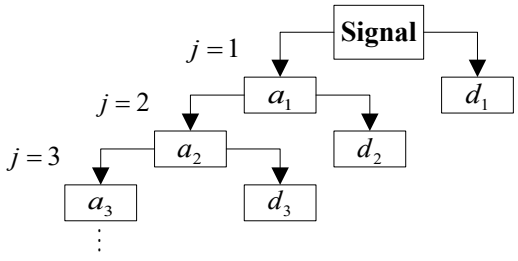

Fig. 1. Discrete wavelet decomposition.

For optimal wavelet function determination, the Daubechies wavelets have been widely employed for many situations, e.g., db2 and db8 for sag detection in [34]. In [35], Symlets and Daubechies wavelets are regarded as optimal ones since they have the highest total wavelet energy. For optimal wavelet decomposition level determination, $j$ has been chosen as 9; see, e.g., [36] for the purpose of feature extraction. For PQ index calculation, a 13-level decomposition has been utilized in [37]. Although DWT and LWT have been widely employed to different applications, they still have limitation, i.e. lack of translation invariance. The reason is provided as follows.

For DWT, the decomposition is performed as follows [38],

$$\begin{cases} a_j(k) = \sum_n h_0(n-2k)a_{j-1}(k), \\ d_j(k) = \sum_n h_1(n-2k)a_{j-1}(k), \end{cases} \tag{3}$$

where $h_1(n)$ and $h_0(n)$ represent for HPF and LPF.

For LWT, the decomposition consists of three steps [39]:

a) Split. Signal $x(k)$ is divided into even samples $x_e(k) = x(2k)$ and odd samples $x_o(k) = x(2k+1)$.

b) Predict.$x_o(k)$ are predicted by $x_e(k)$ and predict operator $P$, with the prediction error $d_j$ defined as

$$d_j(k) = x_o(k) - P \cdot x_e(k). \tag{4}$$

c) Update. In order to obtain $a_j$, $d_j$ is updated by update operator $U$, and then is employed to replace $x_e(k)$,

$$a_j(k) = x_e(k) + U \cdot d_j(k). \tag{5}$$

Due to the down-sampling stage in DWT decomposition and the split step in LWT decomposition, both transforms are lack of translation invariance. The sample size is reduced when the decomposition is performed level by level. To handle this problem, the $\grave{a}trous$ algorithm [29] is introduced:

$$f_j = \begin{cases} f(n), & \text{if } n/2^j \in Z, \\ 0, & \text{otherwise}, \end{cases} \tag{6}$$

where $Z$ stands for the set of integers. In (6), $f_j$ can be substituted by $h_1(n)$ and $h_0(n)$ for DWT. Alternatively, $f_j$ can be substituted by $P$ and $U$ for LWT. The redundant algorithm is also widely adopted with the aim to avoid sample size reduction and information loss; see, e.g., [39].

### C. PQ Disturbances

To realize disturbance classification, the disturbance features are of great significance. Based on the fact that each disturbance has unique features, novel approaches have been reported to realize disturbances classification [40], [41] and complex disturbances detection [35]. In order to provide models for the disturbance-based impact factor analysis in Section III, common PQ disturbances are modeled as follows according to IEEE-1159 Standard [42],

$$S(t) = \begin{cases} cos(2\pi f_C t), t \in (0, t_{start}) \cup (t_{end}, \infty), \\ Acos(2\pi f_C t), t \in [t_{start}, t_{end}], \end{cases} \tag{7}$$

where $t$ is time, $t_{end} - t_{start} \in [0.5, 30]$, (unit cycle omitted) is disturbance duration. $f_C$ is power frequency. Let us define the magnitude of a voltage variation as $\alpha$ and $\alpha = |1 - A|$. For interruption, $A \in [0, 0.1)$. For sag, $A \in [0.1, 0.9]$. For swell, $A \in [1.1, 1.8]$. Three typical disturbances are shown in Fig. 2.

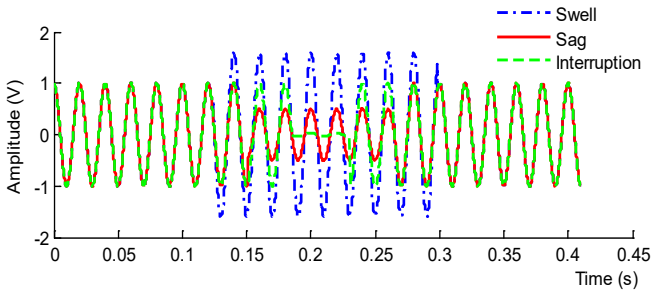


Fig. 2. Disturbance generation: swell, sag and interruption.

## III. Proposed Multiple Impact Factors Analysis

Based on previous works, in order to realize more accurate disturbance location, five impact factors are selected in this paper, and each factor's accuracy impact analysis is explored.

### A. Wavelet Function

Through (3), (4) and (5), it can be seen that as $h_0/h_1$ or $P/U$ varies, wavelets with different properties would be employed for DWT or LWT decomposition, which may lead to distinct analysis results. Unlike wavelet selection for feature extraction [34], [35], this paper explores wavelet function's impact on disturbance location accuracy, due to which optimal wavelet function can be effectively selected. For detailed information of wavelets' properties, readers can refer to Appendix A. For notation simplicity, let us denote compact support by CS, support width by SW, vanishing moments by VM. Common wavelets with distinct properties are given in Table I.

TABLE I
PROPERTIES OF COMMON WAVELET FUNCTION.

| Property | db | coif | Sym | morl | mexh | meyr |
|---|---|---|---|---|---|---|
| Orthogonality | Yes | Yes | Yes | No | No | Yes |
| CS | Yes | Yes | Yes | No | No | No |
| SW | $2N-1$ | $3N-1$ | $2N-1$ | Finite | Finite | Finite |
| DWT | Yes | Yes | Yes | No | No | Yes |
| VM | $N$ | $N$ | $N$ | $N$ | $N$ | $N$ |
| Symmetry | No | No | No | Yes | Yes | Yes |

For the wavelet properties, orthogonality corresponds to tight frame which is useful for signal's energy preservation in the DWT domain, and biorthogonality corresponds to linear phase that can be used to avoid signal distortion. For disturbance detection accuracy that is related with the waveform of a wavelet, these two properties have little impact on disturbance location accuracy, since they have no relation with waveform. Wavelet that has CS, short SW and the ability to perform DWT is more appropriate for industrial applications, since such properties can help save computation cost. Symmetry has no help in transient component capturing. For VM, it determines

the smoothness of a wavelet. As $N$ increases, the wavelet becomes smoother, and the disturbance would be better smoothed according to (1), in which sense the AMM of the located $t_{start}$ and $t_{end}$ would become smaller, making the disturbance detection complicated.

In this sense, to prevent signal from being over smoothed and to save computation cost, the wavelet with medium sized $N$ is more suitable for PQ disturbance detection.

### B. Decomposition Level

Different from the selection of $j$ for feature extraction [36] or disturbance classification [37], the impact of $j$ on disturbance location accuracy is explored in this paper, in that sense the optimal $j$ leading to highest accuracy can be determined.

When decomposition level increases, two scenarios shall appear. First, only $a_j$ is adopted for further decomposition and $d_j$ is left behind, frequency of $a_{j+1}$ and $d_{j+1}$ becomes lower. Second, for classic wavelet, the time window width of wavelet becomes larger. For CWT, through translation and dilation of a mother wavelet $\psi(t)$ whose window width is $\Delta_\psi$, $\psi_{a,b}(t)$'s time window width is $a\Delta_\psi$. For DWT, we have$a = 2^j, b = 2^j k$, andthe time window width of $\psi_{j,k}(t)$ is $2^j\Delta_\psi$. Hence, when $a$ or $j$ increases, $a\Delta_\psi$ or $2^j\Delta_\psi$ increases as well.

Since PQ disturbance can be viewed as a high frequency signal, it can be better represented in high frequency band rather than in the low frequency band. In addition, the wider time window makes the wavelet's focusing capability in time domain weaker, due to which the detection accuracy of sharp variation points in signal is reduced. Hence, it can be deduced that lower decomposition level can help better capture transient components so as to improve disturbance location accuracy.

### C. Redundant Algorithm

Compared to RLWT, DWT and LWT have less redundancy but are lack of translation invariance due to the down-sampling stage as shown in Fig. 1 and the split step. Unlike the redundant algorithm employed to avoid sample size reduction, this paper focuses on the redundant algorithm's solvability of translation invariance and its impact on disturbance location accuracy. In this sense, the algorithm that results in higher location accuracy can be selected accordingly. For a signal $x(k)$ that moves $m$ samples, $x'(k)$ would be obtained as $x(k-m)$. It can be deduced that if $m$ is an odd number, after the down-sampling stage in DWT or the split step in LWT, the samples of $x'(k)$ utilized for $h_0/h_1$ or $P/U$ would be distinct to that of $x(k)$, causing the located $t_{start}$ and $t_{end}$ to vary, such that the disturbance location accuracy is reduced. Some information, especially the one related to $t_{start}$ and $t_{end}$, may be missed when the sample size decreases. Hence, RLWT is of superior robustness and can help store more information, through which the disturbance location accuracy can be improved.

### D. Disturbance-based Impact Factor Investigation

Since disturbance features' impact on location accuracy has not been fully investigated in existing works [40], [41], in this paper, three disturbance features, i.e., event type, disturbance intensity, $t_{start}/t_{end}$ are selected as impact factors, and their potential impact on disturbance location accuracy are explored.

When disturbance $S(t)$ occurs, through the convolution operation denoted as $*$, the wavelet transform of $S(t)$ and wavelet function $\psi(t)$, i.e., $W^1S(j,t)$ can be expressed as

$$W^1S(j,t) = j\,\partial\big((1\pm\alpha)\cos(2\pi f_C t) * \int_{-\infty}^{+\infty}\psi(t)\,dt\big)/\partial t, \quad (8)$$

where $t \in [t_{start}, t_{end}]$. Through (8) it can be seen that the disturbance detection is a derivative problem after smoothing, and the AMM of the located $t_{start}/t_{end}$ is related with $\alpha$. For different event types with the same $t_{start}/t_{end}$, once they share the same $\alpha$, the derivative value would be the same, in which sense the same AMM of the detection results would be obtained. Therefore, the event type has no impact on disturbance location accuracy. With respect to disturbance intensity, the larger $\alpha$ is, the larger the AMM of located $t_{start}/t_{end}$ would be, which means the disturbance is flexible to be detected. Since the ideal supply voltage is a sine waveform, disturbance occurring at the peak point of the sine wave has the sharpest variation, which leads to the largest AMM. Disturbance occurring at the zero-crossing has the mildest variation, leading to the smallest AMM. Hence, disturbance occurring at the peak point is easier to be detected compared to that occurs at the zero-crossing.

## IV. Proposed Impact Factors Based Accuracy Analysis Algorithm

To validate each factor's influence on disturbance location accuracy, an accuracy analysis algorithm based on impact factors is proposed in this section.

### A. Impact Factors Based Accuracy Analysis Algorithm for Disturbance Location

Based on Subsection III-A and III-B, and by considering two perspectives, i.e., wavelet analysis and disturbance features, an impact factors based accuracy analysis algorithm is proposed.

This algorithm can be expressed as the flowchart in Fig. 3.

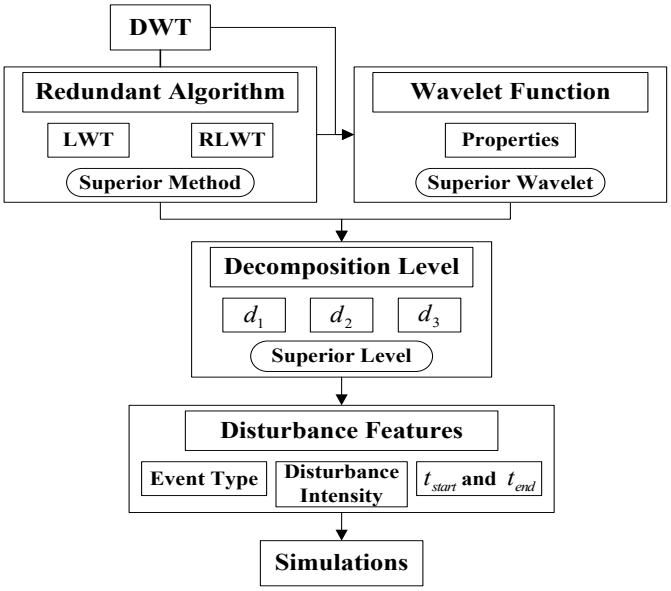

Fig. 3. Impact factors based accuracy analysis algorithm.

Detailed implementation of this algorithm is illustrated as the following five steps:

1. Compare RLWT with DWT and LWT, in which sense the superior method in accuracy improving can be determined.

2. Investigate wavelet function's impact on disturbance location accuracy, such that the superior wavelet would be determined.

3. Employ the superior wavelet to investigate wavelet decomposition's impact on disturbance location accuracy, through which superior lever would be determined.

4. Introduce the superior method, wavelet and decomposition level to investigate the impact of three considered disturbance features including event type, disturbance intensity, $t_{start}$ and $t_{end}$ on disturbance location accuracy, respectively.

5. Implement simulations to validate the above studies.

Then, impact factor investigation on two perspectives, i.e., the wavelet analysis and disturbance features are conducted.

### *B. Wavelet-based Impact Factor Investigation*

#### *(1) Redundant Algorithm*

To explore the potential impact of translation invariance on PQ disturbance location, a comparison scheme is designed:

i. Adopt DWT to obtain corresponding disturbance detection result as $D_{dis}$.

ii. For LWT, due to the split step, two cases are considered:

Case 1: signal's first data sample corresponds to odd sample;

Case 2: signal's first data sample corresponds to even sample.

iii. Employ LWT for both cases to obtain disturbance detection results as $L_{odd}$ and $L_{even}$, respectively. Besides, Employ RLWT for both cases to obtain disturbance detection results as $RL_{odd}$ and $RL_{even}$, respectively.

iv. Utilize $D_{dis}$, $L_{odd}$, $L_{even}$, $RL_{odd}$, $RL_{even}$ for comparison.

#### *(2) Wavelet Function*

Here, the wavelets that shall be adopted for disturbance location analysis are determined. From the perspective of computation cost, the wavelet that has compact support and is able to perform DWT is preferred. Meanwhile, the db and sym wavelets (see Appendix A) have quite similar properties, which can be seen from Table I. So, only adopting one of these two wavelet functions is reasonable. Hence, the db and coif wavelets (see Appendix A) are chosen. Since LWT can be implemented in the time domain [39], the lifting-based wavelet with symmetry is selected. The property differences between the three selected wavelet functions are given in Table II.

TABLE II
PROPERTIES OF THREE DIFFERENT WAVELET FUNCTIONS.

| Property | db | coif | lift |
|---|---|---|---|
| Orthogonality | Yes | Yes | No |
| VM | $N$ | $N$ | $N$ |
| SW | $2N-1$ | $3N-1$ | $4N-3$ |
| Symmetry | No | No | Yes |

It can be seen that the lifting-based wavelet has symmetry and biorthogonality. For the same $N$, the db wavelet has the shortest support width compared to the other two wavelets. Let $N$ vary from 2 to 6 and from 6 to 10, nine wavelets are obtained and are illustrated in Table III, in which Orth stands for Orthogonality, Sym stands for Symmetry. For illustrative purpose, the waveforms of three wavelets with $N = 10$ are shown in Fig. 4.

TABLE III
PROPERTY COMPARISON OF SELECTED WAVELETS.

| Property | db2 | db6 | db10 | coif1 | coif3 | coif5 | lift2 | lift6 | lift10 |
|---|---|---|---|---|---|---|---|---|---|
| Orth | Yes | Yes | Yes | Yes | Yes | Yes | No | No | No |
| VM | 2 | 6 | 10 | 2 | 6 | 10 | 2 | 6 | 10 |
| SW | 3 | 11 | 19 | 5 | 17 | 29 | 5 | 21 | 37 |
| Sym | No | No | No | No | No | No | Yes | Yes | Yes |

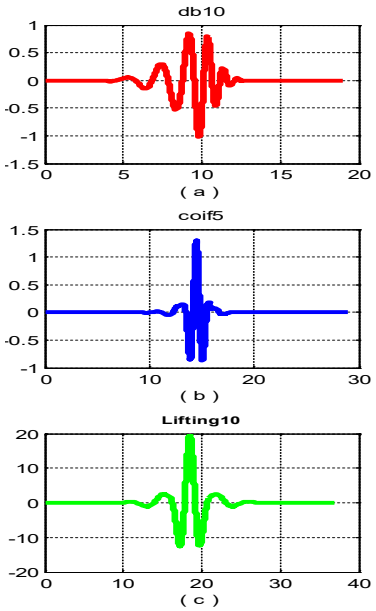


Fig. 4. Waveform of different wavelets: (a) db10; (b) coif5; (c) lift10.

#### *(3) Decomposition Level*

To investigate the optimal decomposition level selection problem, the analysis process is designed as follows:

i. Let $j$ vary from 1 to 3;

ii. Implement $j$-level decomposition to obtain $d_j$;

iii. Compare the modulus maxima of $d_1$, $d_2$, $d_3$.

### *C. Disturbance-based Impact Factor Investigation*

To explore the impact of three disturbance features, i.e., event type, disturbance intensity, $t_{start}$ and $t_{end}$ on disturbance location accuracy, the experimental steps are as follows:

i. Regarding event type, consider both the sag and interruption satisfying $A < 1$ with different $\alpha$ .Two typical events, swell and sag are selected. Then, two groups of disturbance with distinct $t_{start}$ and $t_{end}$ are randomly employed for both swell and sag.

ii. With respect to disturbance intensity, different $\alpha$ is selected for two events. For swell, let us choose $\alpha = 0.5$. For sag, let us choose $\alpha = 0.4$.

iii. To investigate the start and end moments' impact on disturbance detection, two cases are considered:

Case 1: A group of disturbances with changeable $t_{start}$ and fixed $t_{end}$;

Case 2: A group of disturbances with fixed $t_{start}$ and changeable $t_{end}$.

iv. Utilize DWT, LWT and RLWT to detect disturbance.

## V. Simulations

In this section, the simulated signal generated in Matlab and the real signal from the IEEE database [43] are employed to validate each factor's impact on disturbance location accuracy.

### A. Wavelet-based Impact Factors

#### (1) Redundant Algorithm

For illustrative purpose, let us randomly choose a sag of $t_{start} = 0.1732$ and $t_{end} = 0.2825$. LWT and RLWT are applied to both Case 1 and Case 2 in Subsection IV-B, respectively. Disturbance location results are shown in Fig. 5.

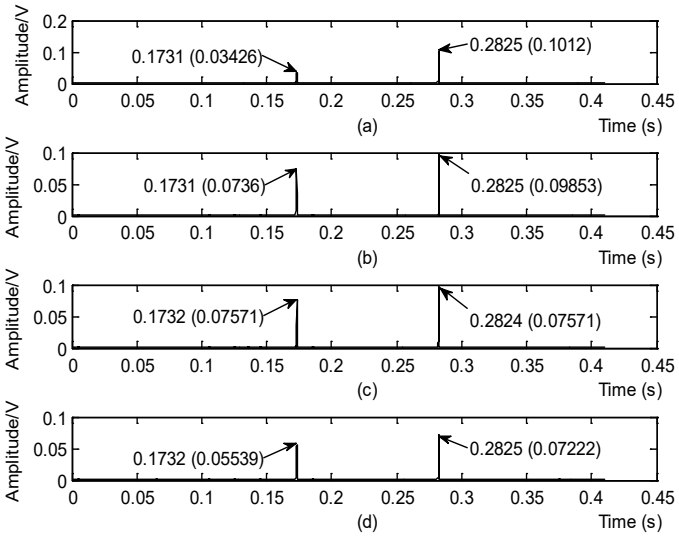


Fig. 5. Redundant algorithm: (a) DWT analysis; (b) LWT for case 1; (c) LWT for case 2; (d) RLWT for both cases.

Fig. 5 shows that through DWT, disturbance location of $t_{end}$ is accurate but fiducial error of 0.0915% happens to $t_{start}$ location. Through LRT, different results are obtained, with disturbance location being 0.1731s and 0.2825s for Case 1, and 0.1732s and 0.2824s for Case 2. A fiducial error of 0.0915% occurs in $t_{start}$ location for Case 1 and in $t_{end}$ location for Case 2, respectively. For RLWT, the same location results are obtained as 0.1732s and 0.2825s for both cases. Meanwhile, disturbance location of both $t_{start}$ and $t_{end}$ are accurate, and the fiducial error are 0%. Hence, the redundant algorithm is verified of superior robustness and better accuracy in disturbance location as compared to DWT and LWT.

#### (2) Wavelet Function

For illustrative purpose, let us randomly choose a sag of $t_{start} = 0.1684$ and $t_{end} = 0.2973$. Then, the nine wavelets in Table III are applied to such disturbance. Disturbance location results through nine wavelets are provided in Table IV.

From Table IV, regarding the relative error between such disturbance and location results of $t_{start}/t_{end}$, the differences among relative error obtained through nine wavelets are minor, and relative error of disturbance duration obtained through nine wavelets are the same. In this sense, symmetry, orthogonality and biorthogonality having little impact on disturbance location accuracy is verified. Nevertheless, as $N$ increases, the AMM of located $t_{start}/t_{end}$ obtained through three wavelet functions decreases monotonically, which verifies that larger $N$ would deduce AMM and make disturbance detection complicated.

TABLE IV.
DISTURBANCE LOCATION THROUGH DIFFERENT WAVELETS.

| Wavelet | $t_{start}$ | AMM | $t_{end}$ | AMM |
|---|---|---|---|---|
| db2 | 0.1683 | 0.1478 | 0.2973 | 0.07462 |
| coif1 | 0.1684 | 0.1315 | 0.2972 | 0.09411 |
| Lift2 | 0.1683 | 0.1317 | 0.2973 | 0.09579 |
| db6 | 0.1684 | 0.1154 | 0.2972 | 0.08008 |
| coif3 | 0.1684 | 0.1136 | 0.2972 | 0.08204 |
| Lift6 | 0.1683 | 0.1129 | 0.2973 | 0.08328 |
| db10 | 0.1683 | 0.09469 | 0.2973 | 0.08351 |
| coif5 | 0.1684 | 0.1076 | 0.2972 | 0.07822 |
| Lift10 | 0.1683 | 0.1071 | 0.2973 | 0.07912 |

Hence, in order to detect disturbance more accurately, the medium-sized $N$ is selected as 4.The db4 wavelet is employed for DWT, and the lift4 wavelet is adopted for LWT and RLWT.

#### (3) Decomposition Level

For illustrative purpose, let us randomly choose a sag of $t_{start} = 0.1538$ and $t_{end} = 0.2742$ for wavelet decomposition at different levels. Disturbance location results through $d_1$, $d_2$ and $d_3$ are shown in Table V.

TABLE V.
DISTURBANCE LOCATION THROUGH DWT AND RLWT AT DIFFERENT LEVELS.

| Algorithm | $d_i$ | $t_{start}$ | $t_{end}$ |
|---|---|---|---|
| DWT | $d_1$ | 0.1538 | 0.2742 |
| | $d_2$ | 0.1536 | 0.2740 |
| | $d_3$ | 0.1539 | 0.2739 |
| RLWT | $d_1$ | 0.1538 | 0.2742 |
| | $d_2$ | 0.1539 | 0.2743 |
| | $d_3$ | 0.1540 | 0.2744 |

Results show that for both DWT and RLWT, the disturbance location errors of $t_{start}/t_{end}$ increase when $j$ becomes larger, which verifies that the increasing of decomposition level would lead to lower disturbance location accuracy. Hence, in the next analysis, $j$ is selected as 1.

### B. Disturbance-based Impact Factors

#### (1) Event Type and Disturbance Intensity

For illustrative purpose, four disturbances are randomly selected: swell 1 and sag 1 with $t_{start} = 0.2436$ and $t_{end} = 0.3163$, swell 2 and sag 2 with $t_{start} = 0.1527$ and $t_{end} = 0.2916$. Disturbance location results are shown in Table VI.

Table VI shows that for both swell and sag with the same $t_{start}$ and $t_{end}$, relative errors of located $t_{start}/t_{end}$ through three transforms are the same, which shows that event type has no impact on disturbance location accuracy. But for both

disturbances, by utilizing any of the three transforms, the AMM of located $t_{start}/t_{end}$ of swell is always larger than that of the sag. Since $\alpha$ is 0.5 for swell and 0.4 for sag, it can be seen that severer disturbance intensity leads to larger AMM of located $t_{start}/t_{end}$, such that the disturbance can be easier detected.

TABLE VI.
LOCATION OF DISTURBANCES WITH DIFFERENT FEATURES.

| Event | Method | $t_{start}$ | AMM | $t_{end}$ | AMM |
|---|---|---|---|---|---|
| Swell 1 | DWT | 0.2435 | 0.034 | 0.3163 | 0.06758 |
| | LWT | 0.2435 | 0.07336 | 0.3163 | 0.06359 |
| | RLWT | 0.2436 | 0.05564 | 0.3162 | 0.0485 |
| Sag 1 | DWT | 0.2435 | 0.0272 | 0.3163 | 0.05406 |
| | LWT | 0.2435 | 0.05869 | 0.3163 | 0.05087 |
| | RLWT | 0.2436 | 0.04451 | 0.3162 | 0.0388 |
| Swell 2 | DWT | 0.1527 | 0.1186 | 0.2915 | 0.07017 |
| | LWT | 0.1527 | 0.1156 | 0.2915 | 0.1495 |
| | RLWT | 0.1527 | 0.08467 | 0.2916 | 0.1108 |
| Sag 2 | DWT | 0.1527 | 0.09487 | 0.2915 | 0.05614 |
| | LWT | 0.1527 | 0.09245 | 0.2915 | 0.1196 |
| | RLWT | 0.1527 | 0.06774 | 0.2916 | 0.08866 |

*(2) The Start and End Moment of Disturbance*

Firstly, a group of disturbances are randomly employed with all $t_{start}$ being 0.188s, and $t_{end}$ are chosen as 0.276s, 0.277s, 0.278s and 0.279s, respectively. Then, another group of disturbances with $t_{start}$ being 0.1006s, 0.1018s, 0.103s and 0.1042s, and all $t_{end}$ being 0.3641s are selected. Both groups of disturbance detection results are shown in Table VII.

TABLE VII.
LOCATION OF DISTURBANCES WITH DIFFERENT START AND END MOMENT.

| Group | Method | $t_{start}$ | AMM | $t_{end}$ | AMM |
|---|---|---|---|---|---|
| 1 | DWT | 0.1879 | 0.05195 | 0.2759 | 0.01992 |
| | | 0.1879 | 0.05195 | 0.2769 | 0.03778 |
| | | 0.1879 | 0.05195 | 0.2779 | 0.05195 |
| | | 0.1879 | 0.05195 | 0.2789 | 0.06102 |
| | RLWT | 0.1879 | 0.08033 | 0.2759 | 0.02995 |
| | | 0.1879 | 0.08033 | 0.2769 | 0.05798 |
| | | 0.1879 | 0.08033 | 0.2779 | 0.08033 |
| | | 0.1879 | 0.08033 | 0.2789 | 0.09481 |
| 2 | DWT | 0.1005 | 0.06297 | 0.3641 | 0.0414 |
| | | 0.1017 | 0.05408 | 0.3641 | 0.0414 |
| | | 0.1029 | 0.0376 | 0.3641 | 0.0414 |
| | | 0.1042 | 0.01676 | 0.3641 | 0.0414 |
| | RLWT | 0.1006 | 0.09863 | 0.3641 | 0.02995 |
| | | 0.1018 | 0.08558 | 0.3641 | 0.02995 |
| | | 0.103 | 0.06051 | 0.3641 | 0.02995 |
| | | 0.1042 | 0.02694 | 0.3641 | 0.02995 |

It can be seen that for the first group of disturbances, the AMM of the located $t_{start}$ and $t_{end}$ appears to have the same changing trend, i.e., the AMM of located $t_{start}/t_{end}$ increases with the change of $t_{end}$. For the second group of disturbances, the AMM obtained through both DWT and RLWT still appears to have the same changing trend, i.e., the AMM of located $t_{start}$ and $t_{end}$ decreases with the change of $t_{start}$.

Hence, simulation results demonstrate that when $t_{start}/t_{end}$ moves from the zero-crossing to the peak point of the sine wave, the AMM of located $t_{start}/t_{end}$ becomes larger, and vice versa.

## C. Case Study

*(1) Real Signal Analysis*

To better verify the above discussion, the real sag signal from IEEE database [36] is employed. The sampling frequency is 20,000Hz, and the sample size is 20,400.

Firstly, DWT, LWT and RWLT are utilized for comparison analysis. Experimental results are obtained in Fig. 6.

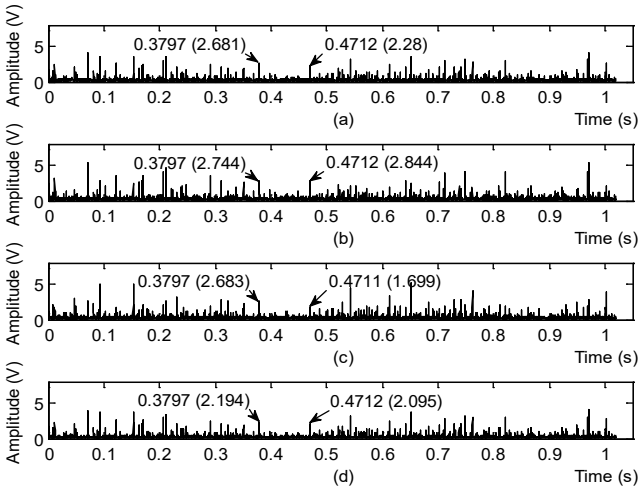


Fig. 6. Comparison of DWT, LWT and RLWT: (a) DWT analysis; (b) LWT for case 1; (c) LWT for case 2; (d) RLWT for both cases.

Results show that locations of $t_{start}$ and $t_{end}$ through DWT and RLWT are the same. However, RLWT is independent of convolution operation and can be realized in the time domain, which requires less computation cost compared to that of DWT. In addition, the located disturbance moments through LWT for two cases in Subsection IV-B are different. For RLWT, same results are obtained. In this sense, it is verified that RLWT has better robustness with respect to disturbance location.

Then, wavelets with different $N$, i.e., lift2, lift4 and lift8 are applied to such real signal. Results are shown in Fig. 7.

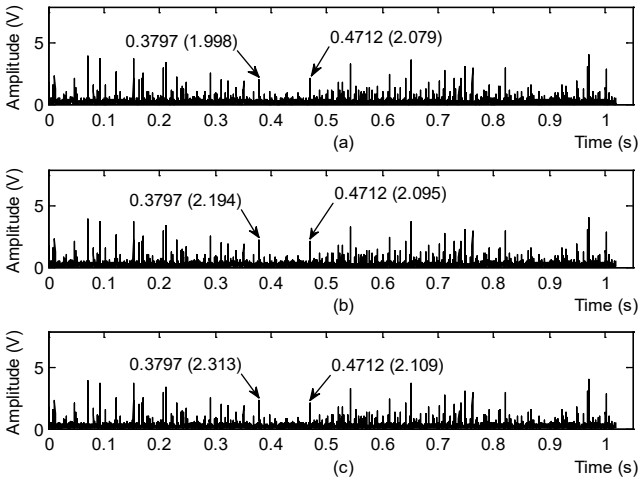

Fig. 7. Disturbance location with different wavelet: (a) lift2; (b) lift4; (c) lift8.

Experimental results show that for wavelets with different $N$, the results of disturbance location are the same, but the AMM of located $t_{start}$ and $t_{end}$ are distinct.

Finally, $j = 1,2,3$ are respectively selected to decompose the signal with lift4. Experimental results are given in Fig. 8.

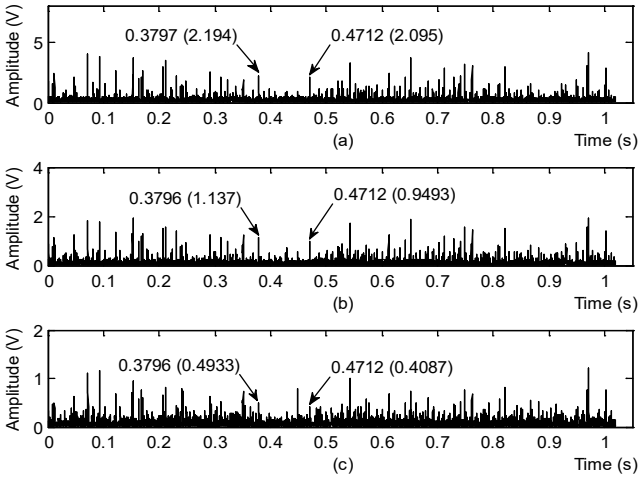


Fig. 8. Disturbance location with different decomposition levels: (a) Analysis result of d1; (c) Analysis result of d2; (d) Analysis result of d3.

It can be seen that as $j$ varies, larger relative error of located $t_{start}$ and $t_{end}$ occurs. In addition, the increase of $j$ also makes AMM decrease, due to which the PQ disturbance location becomes more complicated.

*(2) Analysis of Modeling Signal with Noise*

It is notable that the real sag signal is contaminated by noise which has not been presented in the proposed impact factors based accuracy analysis algorithm. Considering the noise usually exists in the real-world signal, an analysis of modeling signal with noise is implemented in order to further verify the proposed algorithm.

For the purpose of consistency, a sag signal is generated according to Equation 7, with $t_{start}$, $t_{end}$, the sampling frequency and the sample size the same as the real sag signal are. Then, different levels of noise, i.e., SNR of 30dB, 40dB and 50dB are employed, respectively [45], [46].

Firstly, DWT, LWT and RWLT are adopted for comparison analysis, and results are shown in Fig. 9 to Fig. 11. It can be found that for signals at different SNR, same results are obtained as that of the real sag signal: 1) For two cases in Subsection IV-B, the locations of $t_{start}$ and $t_{end}$ through LWT are different, and disturbance location results through RLWT are the same, due to which better robustness of RLWT in disturbance location can be verified. 2) Located disturbance moments through DWT and RLWT are the same. However, compared to DWT, RLWT that is independent of convolution operation requires less computation cost. With respect to different levels of noise, only the AMM of the located disturbance moment may be impacted.

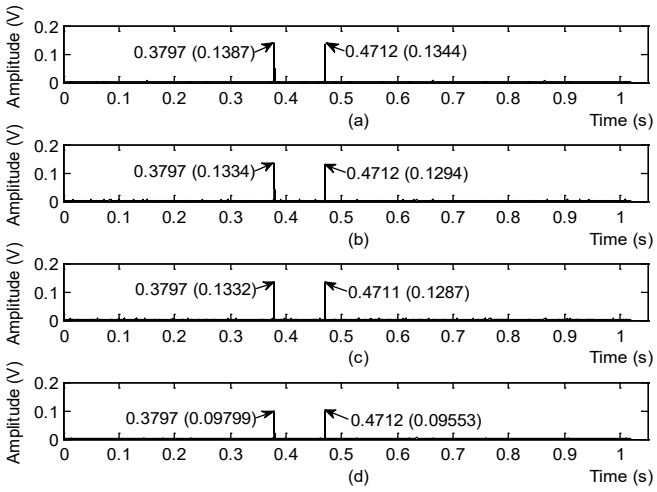


Fig. 9. Comparison of DWT, LWT and RLWT for SNR of 50dB: (a) DWT analysis; (b) LWT for case 1; (c) LWT for case 2; (d) RLWT for both cases.

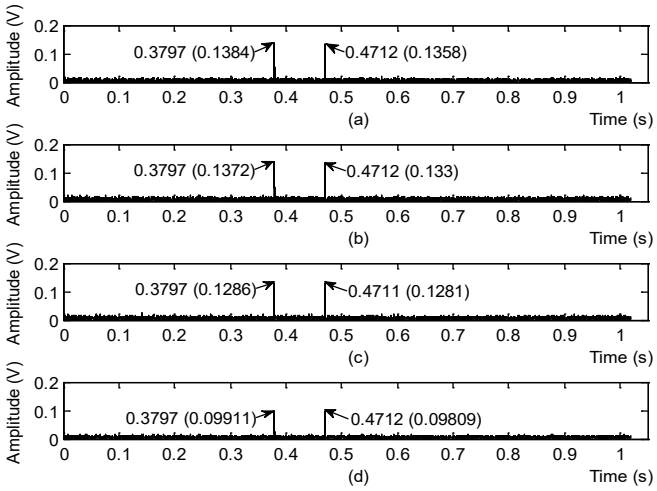


Fig. 10. Comparison of DWT, LWT and RLWT for SNR of 40dB: (a) DWT analysis; (b) LWT for case 1; (c) LWT for case 2; (d) RLWT for both cases.

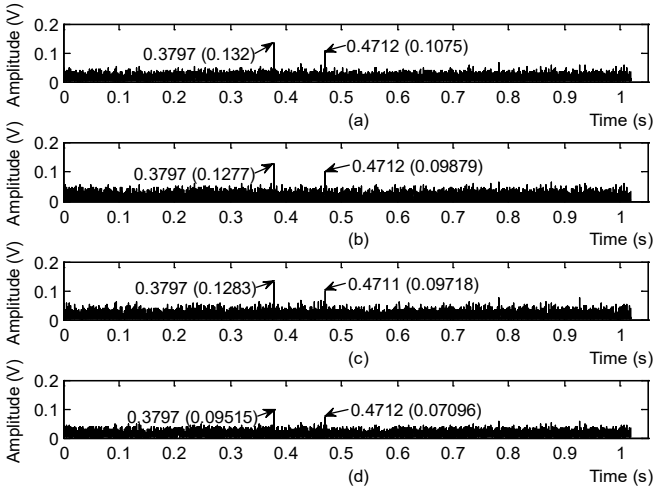

Fig. 11. Comparison of DWT, LWT and RLWT for SNR of 30dB: (a) DWT analysis; (b) LWT for case 1; (c) LWT for case 2; (d) RLWT for both cases.

Then, wavelets with different $\boldsymbol{N}$, i.e., lift2, lift4 and lift8 are utilized to the modeling signal, and experimental results are obtained in Fig. 12 to Fig. 14.

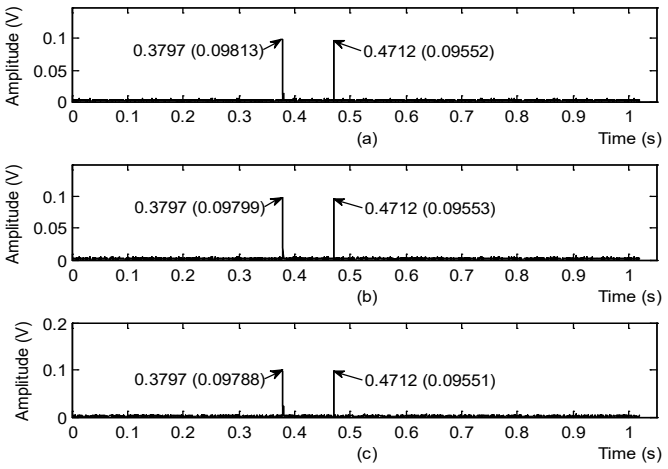


Fig. 12. Disturbance location with different wavelet for SNR of 50dB: (a) lift2; (b) lift4; (c) lift8.

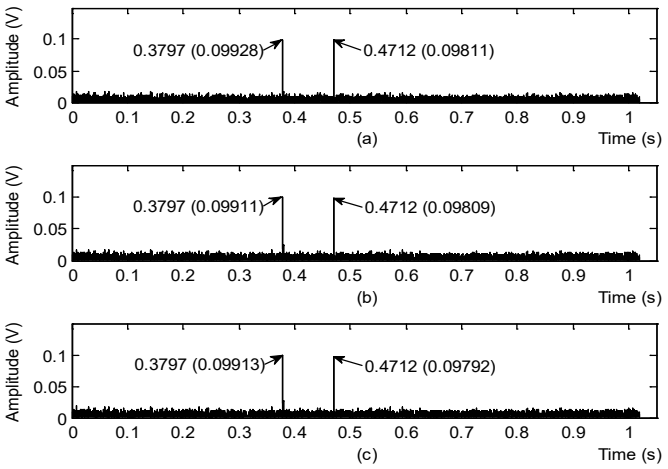


Fig. 13. Disturbance location with different wavelet for SNR of 40dB: (a) lift2; (b) lift4; (c) lift8.

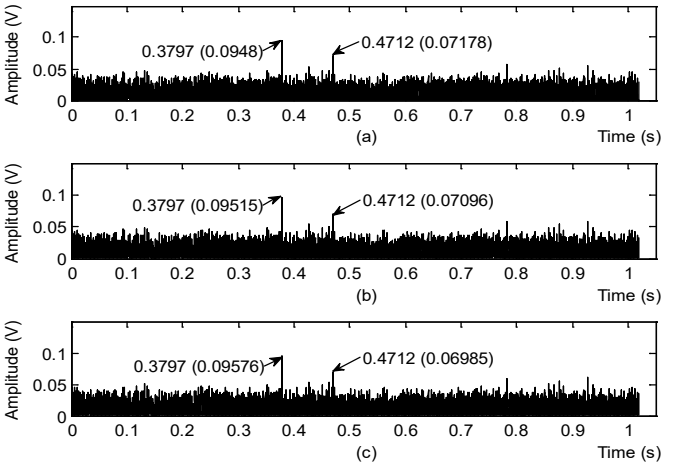


Fig. 14. Disturbance location with different wavelet for SNR of 30dB: (a) lift2; (b) lift4; (c) lift8.

It can be seen that for signals at different SNR, same results are obtained as that of the real sag signal, i.e., through wavelets with distinct $N$, the located $\boldsymbol{t_{start}}$ and $\boldsymbol{t_{end}}$ are the same, only the AMM of located of disturbance moment are distinct.

Finally, $\boldsymbol{j = 1, 2, 3}$ are respectively selected to decompose the modeling signal with lift4, and results are presented in Fig. 15 to Fig. 17.

Experimental results show that for signals at different SNR, larger relative error of located $\boldsymbol{t_{start}}$ and $\boldsymbol{t_{end}}$ would occur with the increase of $\boldsymbol{j}$, which leads to accuracy decrease in disturbance moment location. Different AMM of located disturbance moment would be obtained with the variation of $\boldsymbol{j}$ and SNR. In addition, the amplitude of detailed coefficients of noise decays quickly when j increases, which makes the AMM of located $\boldsymbol{t_{start}}$ and $\boldsymbol{t_{end}}$ easy to be recognized.

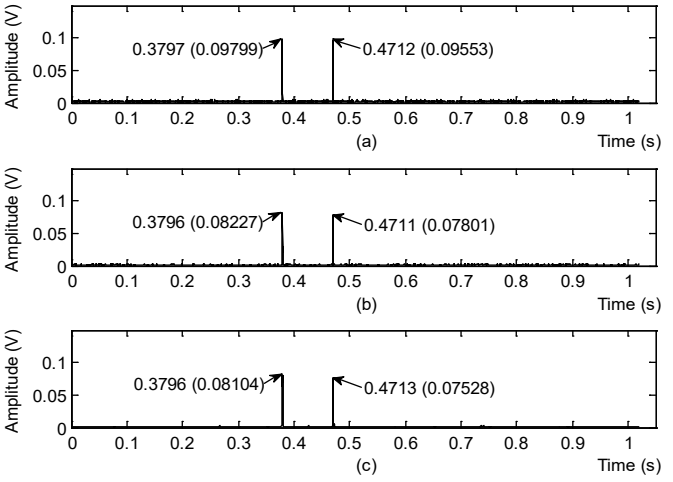


Fig. 15. Disturbance location with different decomposition levels for SNR of 50dB: (a) Analysis result of d1; (c) Analysis result of d2; (d) Analysis result of d3.

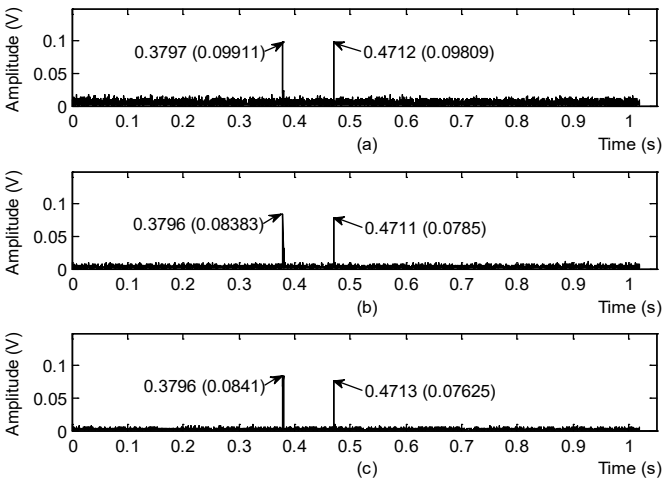


Fig. 16. Disturbance location with different decomposition levels for SNR of 40dB: (a) Analysis result of d1; (c) Analysis result of d2; (d) Analysis result of d3.

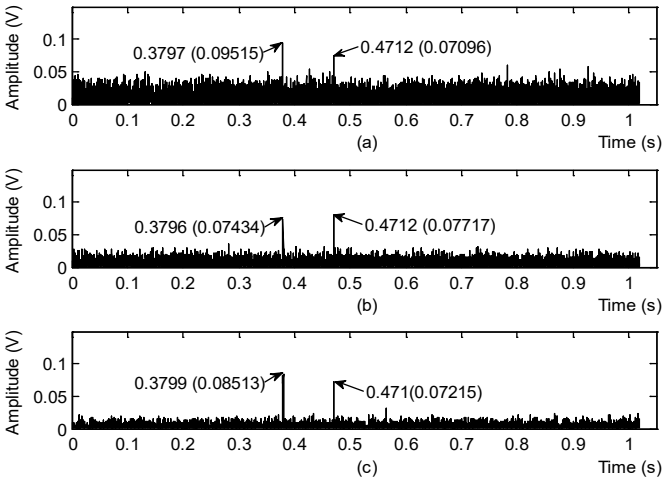


Fig. 17. Disturbance location with different decomposition levels for SNR of 30dB: (a) Analysis result of d1; (c) Analysis result of d2; (d) Analysis result of d3.

From the modeling signal analysis it can be seen that for the real-world applications, i.e., the signal is usually interrupted by noise, different levels of noise would have an impact on the AMM of the located PQ disturbance moment. In addition, as the SNR varies from 50dB to 30dB, i.e., the noise intensity increases, disturbance moment detection becomes complicated due to severer noise pollution. Though the increase of decomposition level can make noise decay on the amplitude of detailed coefficients, the accuracy of PQ disturbance moment location would decrease at the same time.

## VI. Conclusion

This paper focuses on multiple impact factors analysis, with the aim to improve disturbance location accuracy. The impact of five selected factors is analyzed, respectively: 1) Wavelet properties including orthogonality, biorthogonality, symmetry and disturbance feature including event type have little impact on disturbance location accuracy. 2) The decomposition level directly impacts disturbance location accuracy. As $\boldsymbol{j}$ increases, the accuracy decreases. 3) The redundant algorithm has superior robustness to improve disturbance location accuracy. 4) The AMM of located disturbance moment would be impacted by vanishing moments, disturbance intensity and $\boldsymbol{t_{start}/t_{end}}$. It has been verified that when PQ disturbance is detected by wavelet analysis, better location accuracy can be achieved by employing redundant algorithm, wavelet with medium-sized vanishing moments order, or lower $\boldsymbol{j}$.

The restriction of this paper is that though the impact of noise intensity on PQ disturbance detection is investigated, effective approach for denoising so as to realize flexible disturbance moment location has not been explored. In addition, the hardware realization of novel approaches for effective real-time PQ disturbance detection is of great importance. However, the hardware implementation of the proposed multiple impact factors based accuracy analysis for PQ disturbance detection in noise environment needs further investigation, in which the computation cost related key parameters, e.g., execution time sampling frequency need to be carefully considered. In our future work, we shall develop novel approaches to reduce noise, such that PQ disturbance can be detected more flexibly.

## Appendix

Here, some preliminaries of wavelet are introduced briefly. Readers can refer to [44] for further details.

### *A. A Brief Introduction to Wavelet*

For mother wavelet $\boldsymbol{\psi(t)}$ that is processed by dilation factor $a$ and translation factor$b$, the function family $\{\psi_{a,b}\}$ generated

$$\psi_{a,b}(t) = \left|a^{-\frac{1}{2}}\right| \psi\left(\frac{t-b}{a}\right).$$

is defined as wavelet basis.

Due to different properties such as orthogonality, compact support and vanishing moments, various sets of $\{\psi_{a,b}\}$ are employed for different applications. Several common wavelets are: Daubechies, Coiflets, Symlets, Morlet, mexh, Meyer etc. These wavelets can be abbreviated as db, coif, sym, morl, mexh, meyr, respectively. For vanishing moment order that is $N$, Daubechies, Coiflets, Symlets can be simply represented as $dbN$, $coifN$, $symN$, respectively. In this sense, the Daubechies wavelet that has fourth-order or tenth-order vanishing moment is expressed as db4 or db10, respectively.

Based on the lifting algorithm and interpolation subdivision method, the lifting-based wavelet can be constructed. For vanishing moment order that is $N$, the lifting-based wavelet can be simply represented as lift$N$. So, lift2, lift4, lift6, lift8, lift10 express the wavelet has second-order, fourth-order sixth-order, eighth-order, tenth-order vanishing moments, respectively.

## ACKNOWLEDGMENT

This work is supported by the National Natural Science Foundation of China (Grant No.61501040), Beijing Key Laboratory of Digital Printing Equipment, National Key Research and Development Program of China (Grant No. 2017YFE0132100) and BNRist Program (Grant No. BNR2020TD01009).

## REFERENCES

[1] J. Rifkin, "The third industrial revolution: how lateral power is transforming energy, the economy, and the world," Palgrave Macmillan, New York, pp. 31-46, 2013.

[2] H. Hua, J. Cao, G. Yang, and G. Ren, "Voltage control for uncertain stochastic nonlinear system with application to energy Internet: Non-fragile robust $H_\infty$approach," *J. Math. Anal. Appl.*, vol. 463, no. 1, pp. 93-110, 2018.

[3] L. Tang, X. Dong, S. Luo,S. Shi, and B. Wang, "A new differential protection of transmission line based on equivalent travelling wave," *IEEE Trans. Power Delivery*, vol. 32, no. 3, pp. 1359-1369, Jun. 2017.

[4] X. Liang, "Emerging power quality challenges due to integration of renewable energy sources," *IEEE Trans. Ind. Appl.*, vol. 53, no. 2, pp. 855-866, Mar-Apr. 2017.

[5] P. A. Karafotis and P. S. Georgilakis, "Power quality monitoring and evaluation in power systems under non-stationary conditions using wavelet packet transform," *High Volt.*, vol. 4, no. 3, pp. 186-196, Sep. 2019.

[6] H. Chen,P. D. S. Assala, Y. Cai, and P. Yang, "Intelligent transient over voltages location in distribution systems using wavelet packet decomposition and general regression neural networks," *IEEE Trans. Ind. Inform.*, vol. 12, no. 5, pp. 1726-1735, Oct. 2016.

[7] M. Emmanuel, R. Rayudu, and I. Welch, "Impacts of power factor control schemes in time series power flow analysis for centralized PV plants using wavelet variability model," *IEEE Trans. Ind. Inform.*, vol. 13, no. 6, pp. 3185-3194, Dec. 2017.

[8] X. Zheng, Y.Tang, and J. Zhou, "A framework of adaptive multiscale wavelet decomposition for signals on undirected graphs," *IEEE Trans. Signal Process*, vol.67, no. 7, pp. 1696-1711, Apr. 2019.

[9] N. Holighaus, G. Koliander, Z. Prusa, and L. D. Abreu, "Characterization of analytic wavelet transforms and a new phaseless reconstruction algorithm," *IEEE Trans. Signal Process*, vol. 67, no. 15, pp.3894-3908, Aug. 2019.

[10] E. Guillén-García, L. Morales-Velazquez, A. L. Zorita-Lamadrid, O. Duque-Perez, R. A. Osornio-Rios, R. D. J. Romero-Troncoso, "Accurate identification and characterization of transient phenomena using wavelet transform and mathematical morphology," *IET Gener. Transm. Dis*, vol. 13, no. 18, pp. 4021-4028, Sep. 2019.

[11] N. Ansari and A. Gupta, "M-RWTL: learning signal-matched rational wavelet transform in lifting framework," *IEEE Access*, vol. 6, pp. 12213-12227, Jan. 2018.

[12] A. Roy and A. P.Misra, "Audio signal encryption using chaotic Hénon map and lifting wavelet transforms," Springer Berlin Heidelberg, Berlin, 2017.

[13] K. Thirumala, Shantanu, T. Jain, and A. C. Umarikar, "Visualizing time-varying power quality indices using generalized empirical wavelet transform," *Electr. Pow. Syst. Res,*, vol. 143, pp. 99-109, Feb. 2017.

[14] B. Abhijit and P. B. Ram, "A Multivariate approach for patient-specific EEG seizure detection using empirical wavelet transform," *IEEE Trans. Bio-Med. Eng.*, vol. 64, no. 9, pp. 2003-2015, Sep. 2017.

[15] K. Thirumala, A. C. Umarikar, and T. Jain, "Estimation of single-phase and three-phase power-quality indices using empirical wavelet transform," *IEEE Trans. Power Deliv.*, vol. 30, no. 1, pp. 445-454, Feb. 2015.

[16] R. Kumar, B. Singh, D. T. Shahani, and C. Jain, "Dual-tree complex wavelet transform-based control algorithm for power quality improvement in a distribution system," *IEEE Trans. Ind. Electron.*, vol. 64, no. 1, pp. 764-772, Jan. 2017.

[17] P. K. Ray, N. Kishor, and S. R. Mohanty, "Islanding and power quality wavelet and S-transform," *IEEE Trans. Smart Grid*, vol. 3, no. 3, pp. 1082-1094, Sept. 2012.

[18] Z. Liu, Q.Hu,Y. Cui, and Q. Zhang, "A new detection approach of transient disturbances combining wavelet packet and Tsallis entropy". *Neurocomputing*, vol. 142, pp. 393-407, Oct. 2014.

[19] F. Hafiz, A. Swain, C. Naik, S. Abecrombie and A. Eaton, "Identification of power quality events: selection of optimum base wavelet and machine learning algorithm," *IET Sci., Meas., Technol.*, vol. 13, no. 2, pp. 260-271, Mar. 2019.

[20] S. A. Deokar and L. M. Waghmare, "Integrated DWT-FFT approach for detection and classification of power quality disturbances," *Elec. Power & Energy Syst.*, vol. 61, pp. 594-605, Oct. 2014.

[21] B. Biswal and S. Mishra, "Power signal disturbance identification and classification using a modified frequency slice wavelet transform,"*IET Gener. Transm.,* vol. 8, no. 2, pp. 353-362, Feb. 2014.

[22] S. Khokhar, A. A. Mohdzin, A. P. Memon, and A. S.Mokhtar, "A new optimal feature selection algorithm for classification of power quality disturbances using discrete wavelet transform and probabilistic neural network," *Measurement*, vol. 95, pp. 246-259, Jan. 2017.

[23] M. K. Saini, R. K. Beniwal, "Optimum fractionally delayed wavelet design for PQ event detection and classification," *Int. Trans. Electr. Energy*, vol. 27, no. 10, Oct. 2017.

[24] B. Eristi, O. Yildirim, H. Eristi and Y. Demir, "A new embedded power quality event classification system based on the wavelet transform," *Int. Trans. Electr. Energy*, vol. 28, no. 9, Sep. 2018.

[25] D. K. Alves, F. B. Costa, R. Lucio De Araujo Ribeiro, C. Martins De Sousa Neto and T. De Oliveira Alves Rocha, "Real-time power measurement using the maximal overlap discrete wavelet-packet transform," *IEEE Trans. Ind. Electron.*, vol. 64, no. 4, pp. 3177-3187, Apr. 2017.

[26] Y. Zhang, T. Ji, M. Li and Q. Wu, "Identification of power disturbances using generalized morphological open-closing and close-opening undecimated wavelet," *IEEE Trans. Ind. Electron.*, vol. 63, no. 4, pp. 2330-2339, Apr. 2016.

[27] Z. Liu, Z. Han, Y. Zhang, and Q. Zhang, "Multiwavelet packet entropy and its application in transmission line fault recognition and classification," *IEEE Trans. Neural Networks and Learning Syst.*, vol. 25, no. 11, pp. 2043-2052, Nov. 2014.

[28] J. Chen and G. Li, "Tsallis wavelet entropy and its application in power signal analysis". *Entroypy*, vol.16, no. 6, pp. 3009-3025, Jun. 2014.

[29] T. Zafar and W.G. Morsi, "Power quality and the un-decimated wavelet transform: an analytic approach for time-varying disturbances," *Elect. Power Syst. Res.*, vol. 96, pp. 201-210, Mar. 2013.

[30] V. K. Tiwari and S. K. Jain, "Hardware implementation of polyphase-decomposition-based wavelet filters for power system harmonics estimation," *IEEE Trans. Instrum. Meas.*, vol. 65, no. 7, pp. 1-11, Jul. 2016.

[31] D. Bayram and S. Seker, "Redundancy-based predictive fault detection on electric motors by stationary wavelet transform," *IEEE Trans. Industry Applications*, vol. 53, no. 3, pp. 2997-3004, May-Jun. 2017.

[32] K. Thirumala, P. M. Siva, T. Jain, and A. C. Umarikar, "Tunable-Q wavelet transform and dual multiclass SVM for online automatic detection of power quality disturbances source," *IEEE Trans. Smart Grid*, vol. 9, no. 4, pp. 3018-3028, Jul. 2018.

[33] P. Kanirajan and K. V. Suresh, "Power quality disturbance detection and classification using wavelet and RBFNN," *Appl. Soft Comput.*, vol. 35, pp. 470-481, Jul. 2015.

[34] M. B. Latran and A.Teke, "A novel wavelet transform based voltage sag/swell detection algorithm," *Int. J Electr. Power Energy Syst.*, vol. 71, pp. 131-139, Oct. 2015.

[35] F. B. Costa, "Boundary wavelet coefficients for real-time detection of transients induced by faults and power-quality disturbances," *IEEE Trans. Power Delivery*, vol. 29, no. 6, pp. 2674-2687, Dec. 2014.

[36] H. Eristi, Ö. Yildirim, B. Eristi, and Y. Demir, "Optimal feature selection for classification of the power quality events using wavelet transform and least squares support vector machines," *Int. J. Electr. Power Energy Syst.*, vol. 49, no. 1, pp. 95–103, Jul. 2013.

[37] C. A. Naik and P.Kundu, "Power quality index based on discrete wavelet transform,"*Elec. Power & Energy Syst.*, vol. 53, pp. 994-1002, Dec. 2013.

[38] L. Xiong, X. Zhong, and C. Yang, "DWT-SISA: a secure and effective discrete wavelet transform-based secret image sharing with authentication," *Signal Process.*, vol.173, Aug. 2020.

[39] Z. Yang, L. Cai, L. Gao, and H. Wang, "Adaptive redundant lifting wavelet transform based on fitting for fault feature extraction of roller bearings," *Sensors*, vol. 12, no. 4, pp. 4381-4398, Apr. 2012.

[40] F. A. S. Borges, R. A. S. Fernandes, I. N. Silva, and B. S. Cíntia, "Feature extraction and power quality disturbances classification using smart

meters signals," *IEEE Trans. Ind. Inform.*, vol. 12, no. 2, pp. 824-833, Apr. 2016.
[41] Z. Liu, Y. Cui, and W. Li, "A classification method for complex power quality disturbances using EEMD and rank wavelet SVM," *IEEE Trans. Smart Grid*, vol. 6, no. 4, pp. 1678-1685, Jul. 2015.
[42] I. Standard, IEEE Recommended Practice for Monitoring Electric Power Quality, IEEE Std 1159-2019, Institute of Electrical and Electronics Engineers, NewYork, USA, 2019, pp. 1-98.
[43] https://ieee-dataport.org/documents/real-life-power-quality-sags.
[44] A. R. Adly, Aleem, H. E A. Shady, M. A. Algabalawy, MA, F. Jurado, F, and Z. M. Ali, "A novel protection scheme for multi-terminal transmission lines based on wavelet transform," *Electr. Pow. Syst. Res.*, vol.183, Jun. 2020.
[45] T. Zhong, S. Zhang, G. Cai, Y. Li, B. Yang, and Y. Chen, "Power Quality Disturbance Recognition Based on Multiresolution S-Transform and Decision Tree," *IEEE Access*, vol. 7, pp. 88380-88392, Jun. 2019.
[46] R. Kumar, B. Singh, R. Kumar, and S. Marwaha, "Recognition of underlying causes of power quality disturbances using stockwell transform," *IEEE Trans. Instrum. Meas.*, vol. 69, no. 6, pp. 2798-2807, Jun. 2020.

ZijingYang was born in Hunan, P. R. China in 1984. She received her Ph.D. in mechanical engineering from the University of Technology in 2012.From 2012 to 2014, she was a Postdoctoral Fellow in the Research Institute of Information Technology, Tsinghua University, Beijing, P. R. China. She is currently the Vice Director of Beijing Key Laboratory of Digital Printing Equipment, Beijing Institute of Graphic Communication, Beijing, China. Her research focuses on signal processing technology, and its applications in smart grid and fault diagnosis.

Haochen Hua was born in Jiangsu, P. R. China in 1988. He received the B.Sc. degree in mathematics with finance in 2011, and the Ph.D. degree in mathematical sciences in 2016, both from the University of Liverpool, Liverpool, UK. From 2016 to 2020, he was a Postdoctoral Fellow in the Research Institute of Information Technology, Tsinghua University, Beijing, P. R. China. Since 2020, he has been a Professor in the College of Energy and Electrical Engineering, Hohai University, Nanjing, P. R. China. His current research interests include optimal and robust control theory and its applications in power systems, smart grids, and the energy internet.

Junwei Cao received his Ph.D. in computer science from the University of Warwick, Coventry, UK, in 2001. He received his bachelor and master degrees in control theories and engineering in 1998 and 1996, respectively, both from Tsinghua University, Beijing, China. He is currently Professor and Vice Dean of Research Institute of Information Technology, Tsinghua University, Beijing, China. He is also Director of Open Platform and Technology Division, Tsinghua National Laboratory for Information Science and Technology.

Prior to joining Tsinghua University in 2006, he was a Research Scientist at MIT LIGO Laboratory and NEC Laboratories Europe for about 5 years. He has published over 200 papers and cited by international scholars for over 18,000 times. He has authored or edited 8 books. His research is focused on distributed computing technologies and energy/power applications.

Prof. Cao is a Senior Member of the IEEE Computer Society and a Member of the ACM and CCF.